

Diabetes mellitus modeling and short-term prediction based on blood glucose measurements

F. Ståhl, R. Johansson *

Department of Automatic Control, Lund University, P.O. Box 118, SE22100 Lund, Sweden

ARTICLE INFO

Article history:

Received 21 January 2008

Received in revised form 24 September 2008

Accepted 6 October 2008

Available online 30 October 2008

Keywords:

Diabetes

Mathematical model

System identification

Predictor

Glucose dynamics

Insulin dynamics

ABSTRACT

Insulin-Dependent Diabetes Mellitus (IDDM) is a chronic disease characterized by the inability of the pancreas to produce sufficient amounts of insulin. Daily compensation of the deficiency requires 4–6 insulin injections to be taken daily, the aim of this insulin therapy being to maintain normoglycemia – i.e., a blood glucose level between 4 and 7 mmol/l. To determine the quantity and timing of these injections, various different approaches are used. Currently, mostly qualitative and semi-quantitative models and reasoning are used to design such a therapy. Here, an attempt is made to show how system identification and control may be used to estimate predictive quantitative models to be used in design of optimal insulin regimens.

The system was divided into three subsystems, the insulin subsystem, the glucose subsystem and the insulin–glucose interaction. The insulin subsystem aims to describe the absorption of injected insulin from the subcutaneous depots and the glucose subsystem the absorption of glucose from the gut following a meal. These subsystems were modeled using compartment models and proposed models found in the literature. Several black-box models and grey-box models describing the insulin/glucose interaction were developed and analyzed. These models were fitted to real data monitored by an IDDM patient. Many difficulties were encountered, typical of biomedical systems: Non-uniform and scarce sampling, time-varying dynamics and severe nonlinearities were some of the difficulties encountered during the modeling. None of the proposed models were able to describe the system accurately in all aspects during all conditions. However, all the linear models shared some dynamics. Based on the estimated models, short-term blood glucose predictors for up to two-hour-ahead blood glucose prediction were designed. Furthermore, we explored the issues that arise when applying prediction theory and control to short-term blood glucose prediction.

© 2008 Elsevier Inc. All rights reserved.

1. Preface

In January 2002, the first author was diagnosed with Diabetes Type 1 and soon realized the difficulty of maintaining normoglycemia. The question was raised whether control theory could be applied to the problem. To analyze the system using methods of control theory, a model of the system is essential. This paper is an attempt to estimate such a model based on home-monitored data, typically found in a diabetes diary. The models used were primarily linear and were found to be partly insufficient to describe the system.

2. Introduction

Diabetes Mellitus is a disease characterized by the inability of the pancreas to produce sufficient amounts of insulin. To cover

the deficiency 4–6 insulin injections have to be taken daily, the aim being to keep the blood glucose level as constant as possible. To determine the amount and timing of these injections different approaches are used. Mostly qualitative and semi-quantitative models and reasoning are used to design such a therapy. Most patients monitor their blood glucose using personal glucose meters, and determine their own insulin injections based on these results. Poorly controlled blood glucose levels may result in severe complications. Hypoglycemia – i.e., low blood glucose levels – may lead to brain damage [2], coma and eventually death. On the other hand, hyperglycemia – i.e., high blood glucose levels – can result in chronic damages such as retinopathy, kidney failure and amputation due to angiopathy. All patients set their own insulin regime with aid from their physician based on HbA_{1c} , personal observations and a qualitative estimate of the glucose data. These regimes are to their nature rigid and non-flexible. They form the basis for the therapy and patients often have to – and are encouraged to – alter their injection doses when their behavior deviate from the routine the regime was based on. In these situations, the patients

* Corresponding author. Tel.: +4646 222 8791; fax: +4646 138118.

E-mail address: Rolf.Johansson@control.lth.se (R. Johansson).

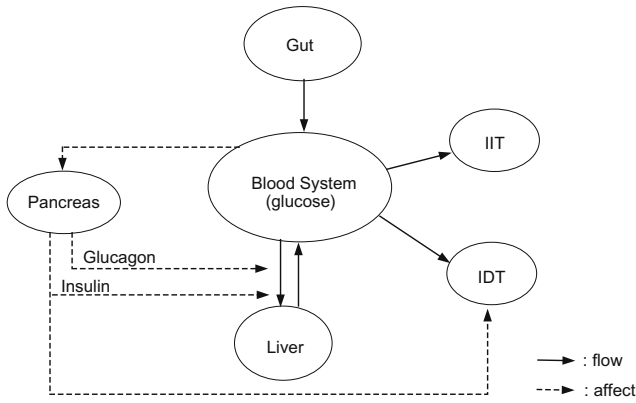


Fig. 1. Overview of the glucoregulatory system. IIT, insulin independent tissue; IDT, insulin-dependent tissue.

have to rely on their own knowledge and understanding of the disease to correct their doses. Many patient would benefit from some sort of decision support in these situations. Such a tool would require a model of the effect of regime changes on blood glucose levels. This paper addresses the question of how such models could be retrieved from patient data.

The glucoregulatory system controls glucose metabolism and the insulin/glucose mechanisms needed to maintain normoglycemia [3–6]. Fig. 1 shows a simplified overview of the flow of glucose and insulin between the most important organs relevant for this system is shown. For modeling purposes, the system is considered to consist of three main parts: the Glucose Sub-Model (GSM), the Insulin Sub-Model (ISM) and the Glucose/Insulin interaction Model (GIIM). The GSM describes the absorption of glucose from meal, the ISM the absorption of insulin from insulin injections and the GIIM the interaction of glucose and insulin in the blood system and organs (Fig. 2). These three parts will be modeled separately using mainly compartment models and linear black-box models [7,8]. In addition, several previous quantitative approaches to data-based modeling exist [9–14]. In particular, Sparacino et al. [12] presented low-complexity prediction strategies (prediction horizon 30 min) based on continuous blood glucose measurement. The purpose of this paper is to evaluate various different data-based modeling approaches to Diabetes Mellitus. Based on daily monitoring of blood glucose, these models will be used for prediction of future blood glucose values as support for determination of insulin therapy. To find the best model, various different model validation criteria will be used [8, Chapter 9]. Given data on present and previous blood glucose values, the aim was to predict the glycemic behavior for the next 2 h with a reasonable accuracy. This target accuracy was defined as a standard deviation of the prediction error less than 0.5 mmol/l. Although cross validation was used, the models were estimated and validated using primarily one patient's data. It would be preferable to validate the models using other patients' data as well, but due to the scarcity of data this was not possible. This is of course a significant limitation, which has to be regarded when evaluating the validity of the models.

3. Methods and experimental conditions

The blood glucose data primarily used in this paper were collected during the first six months of a newly diagnosed type-1 patient. The glucose testing was undertaken using a personal blood glucose tester, Accu-check Compact, Roche Diagnostics [32]. Meals, insulin injections and glucose samples were noted and registered in a diary (Fig. 3).

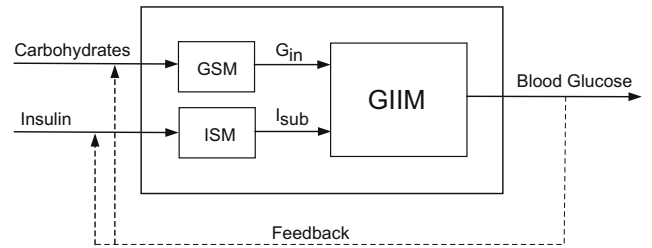


Fig. 2. The partitioning of the system.

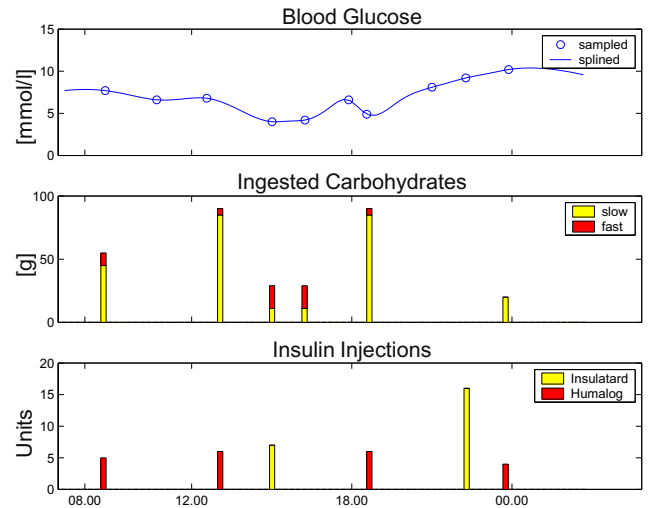


Fig. 3. Diary of insulin intake, ingested carbohydrates, and blood glucose samples during a typical day.

3.1. Non-uniform sampling and data reconstruction

The glucose sampling was based on a sampling schedule following the daily routine. To capture the rapid dynamics caused by the intake of carbohydrates, samples were taken before and 1.5 h after each meal. Sampling was also scheduled at the late Insulatard injection. Additional to these measurements further unscheduled samples were collected, making the average sampling frequency 9.3 samples/day.

Whereas the data were infrequently and non-uniformly sampled, the identification methods used here require uniformly sampled data. To fulfill this demand, spline interpolation of the data were used. To avoid under- and overshoot artefacts caused by the splines, linearly interpolated help spots were added to the original data, a method used in [16] as well. In order for these spots not to influence the spline in a negative way, different weights were assigned the true data and the help spots during the spline interpolation. The time frame was chosen to 15 min intervals, the reason being mainly to accommodate the timing accuracy of meal intake and insulin injections of the diary. For purposes of system identification, removal of outliers, detrending were done as part of standard data pre-processing [8].

3.2. Insulin and carbohydrate modeling

The timing and dose of each injection were noted. The injections were considered to take place instantaneously:

$$u_{IT}(t) = \sum_k D_{IT,k} \cdot \delta(t - t_k) \quad (\text{Insulatard}), \quad (1)$$

$$u_{Hum}(t) = \sum_k D_{Hum,k} \cdot \delta(t - t_k) \quad (\text{Humalog}), \quad (2)$$

where $D_{IT,k}$ and $D_{Hum,k}$ are the Insulatard and Humalog doses (U) at time t_k .

Intake of food was noted semi-quantitatively using predefined meals (Appendix A), each meal being quantified using three levels; small, normal and large, for example:

Time	Food	Type
08.45	Breakfast	Normal
12.30	Lunch	Large
16.00	Snack	Small
18.15	Dinner	Normal

The predefined meals were determined by estimating the composition and size of some standard meals as published by nutritionist [17] with a balance considering carbohydrate intake only. The carbohydrates were divided into two different main types; fast and slow. Mono- and disaccharides were considered fast carbohydrates and the rest were considered slow. All meals were considered to be ingested within 15 min. Thereby the carbohydrate intake can be mathematically expressed as:

$$u_{slow}(t) = \sum_k C_{slow,k} \cdot \delta(t - t_k), \quad \text{Slow carbohydrates,} \quad (3)$$

$$u_{fast}(t) = \sum_k C_{fast,k} \cdot \delta(t - t_k), \quad \text{Fast carbohydrates,} \quad (4)$$

where $C_{slow,k}$ and $C_{fast,k}$ are the amounts [g] of slow and fast carbohydrates ingested at time t_k , respectively. Modeling of metabolic transformation can be approached by means of compartment models – i.e., specialized state-space models – where the structure of the system is postulated, a so-called grey-box model consisting of interacting separate entities, called compartments [7]. Among these compartments energy and material flow as described by different rate constants, c_{ij} . The state-space model identification was approached by various means of system identification such as state-space model identification or ARMAX models [8,21,22,20]. Model validation of the estimated models were made according to statistical model validation criteria including Akaike information criterion (AIC), final prediction error (FPE), minimum description length (MDL), variance accounted for (VAF), root-mean-square error (RMS), residual correlation [8].

4. Modeling of insulin and carbohydrate subsystems

Type-1 diabetics are treated with a therapy with the intention to mimic the normal behavior in a healthy person. Basal injection of slow-acting insulin is taken once or twice a day. It serves to preserve a basal level of insulin required to maintain normal activity. Bolus injections are rapid-acting insulin injections taken to counteract the massive glucose flux following a meal. The slow-acting insulin used here is Insulatard™ and the rapid-acting insulin is Humalog™. Whereas Insulatard™ (Novo Nordisk [42]) is an intermediate/long-lasting insulin of NPH-type, Humalog™ (Lilly [43]) is a rapid-action monomeric insulin. Approximate time-action profiles are provided by the manufacturers and in the review [6].

4.1. The insulin subsystem

The dynamics of insulin is one of the most important factors affecting the outfall of the therapy. Much research is targeted at developing new insulin analogs, both long-lasting and rapid-acting ones. However, the mathematical modeling of the insulin action is still quite poorly developed. Most models are either compartment models or highly sophisticated nonlinear physiological models [6,23]. The compartment models are linear and thereby do not in-

clude the important nonlinearity of dose-dependent dynamics. The nonlinear models, on the other hand, are often too complex to be feasible for routinely use. However, there is one model that has been proposed, that both enhances the simplicity of the compartment models as well as featuring the important nonlinearity of dose-dependent dynamics – i.e., the model proposed by Berger and Rodbard [24]. It will be used here to represent insulin absorption of the slow-acting insulin. The linear relationship between peak time and insulin dose does not exist for rapid-acting insulin. Glucose clamp studies show that the absorption rate is independent of insulin dose in the range 0.05–0.4 U/kg for these insulins [25]. Therefore, these injections will be modeled using a classical compartment model. Together the long-lasting and rapid-acting insulin absorptions form the total insulin flux (Fig. 4):

$$I_{sub}(t) = I_{subIT}(t) + I_{subHum}(t). \quad (5)$$

Insulatard, $I_{subIT}(t)$, was modeled using the Berger model [24]. According to this model the amount of remaining insulin in the depot is:

$$A(t) = 100 - \frac{100 \cdot t^s}{T_{50}^s + t^s}, \quad (6)$$

where T_{50} is the time when half of the dose has been absorbed. The linear dependency between the absorption half-time and dose is expressed as

$$T_{50} = a_{50} \cdot u_{IT}(t) + b_{50}. \quad (7)$$

The rate of absorption is

$$\frac{dA}{dt} = \frac{s \cdot t^s \cdot T_{50}^s}{t \cdot (T_{50}^s + t^s)^2} \cdot u_{IT}(t). \quad (8)$$

Dividing dA/dt with the distribution volume, V yields the insulin absorption rate

$$I_{subIT}(t) = \frac{s \cdot t^s \cdot T_{50}^s}{t \cdot (T_{50}^s + t^s)^2} \cdot u_{IT}(t) = f_{sub}(u_{IT}(t), t) \cdot u_{IT}(t) \quad [\text{mmol}/(\text{liter time})]. \quad (9)$$

The monomeric insulin Humalog, $I_{subHum}(t)$, was modeled according to the compartment model (Fig. 5). Mass balances for each compartment give the following system:

$$\dot{x}^{Hum}(t) = \begin{pmatrix} -c_{11} & 0 \\ c_{21} & -c_{22} \end{pmatrix} x^{Hum}(t) + \begin{pmatrix} 1 \\ 0 \end{pmatrix} u^{Hum}(t), \quad (10)$$

$$I_{subHum}(t) = (0 \quad 1/V)x(t). \quad (11)$$

The transfer function becomes

$$H_{subHum}(s) = C_{Hum} \cdot (s \cdot I - A_{Hum})^{-1} \cdot B_{Hum}, \quad (12)$$

$$= \frac{c_{21} \cdot 1/V}{(s + c_{11}) \cdot (s + c_{22})}. \quad (13)$$

Discretization yields

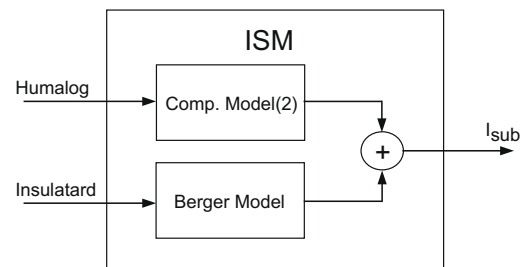


Fig. 4. The insulin sub-model (ISM).

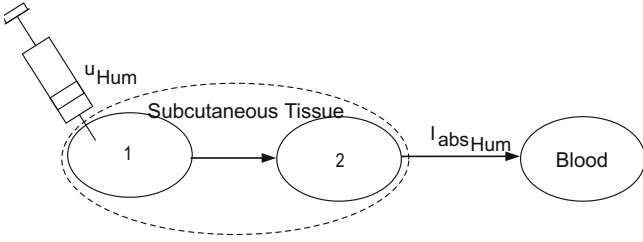


Fig. 5. Compartment model of monomeric insulin.

$$x_{k+1}^{Hum} = \begin{pmatrix} d_{11} & 0 \\ d_{21} & d_{22} \end{pmatrix} x_k^{Hum} + \begin{pmatrix} b_1 \\ b_2 \end{pmatrix} \cdot u_k^{Hum}, \quad (14)$$

$$\Gamma_k^{subHum} = \begin{pmatrix} 0 & 1/V \end{pmatrix} \cdot x_k^{Hum}. \quad (15)$$

Both the glucose and the insulin subsystem dynamics vary significantly between different individuals. Up to 30% of interpersonal variation in the insulin absorption profiles has been reported [28]. Therefore, it is very important to estimate these systems individually. However, identifying these subsystems without tracer experiments is very difficult, and will not be subjected here [34]. Instead, absorption profiles provided by the research literature will be considered. In [6], two estimates of the absorption profile of monomeric insulin can be found. Fitting the compartment model to the M4 profile yielded the following dynamical parameters; $c_{11} = c_{22} = 0.3$. The NPH insulin was modeled using the parameter values found in [6]. In Fig. 6, the simulated injection of 10 U Humalog and 10 U Insulatard can be seen.

4.2. The glucose sub-model

Less attention has been given to the mathematical modeling of the digestive system. In [23], a complex physiological model is derived where the composition of the meal regarding carbohydrates, proteins and fats are considered. In this paper, the model will be kept simple, by only looking at the amount of carbohydrates in each meal. The digestive system will be modeled by a compartment model similar to the model developed in [26]. The gastrointestinal tract is considered consisting of a number of compartments. Each compartment interacts with the neighboring compartments. The flow is one-directional, finally reaching the blood compartment. These compartments can be given various

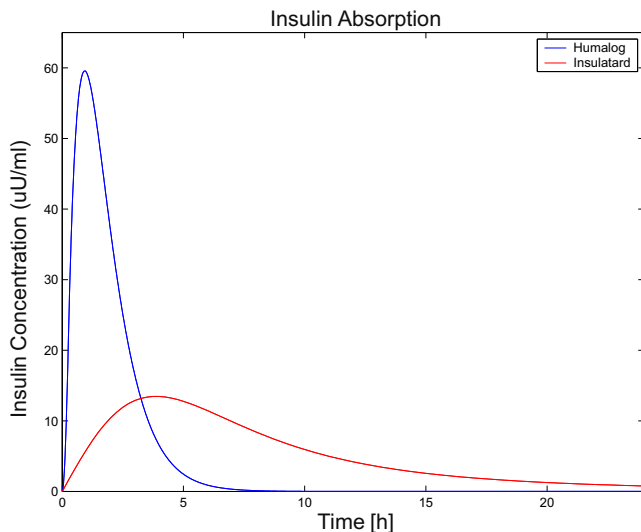


Fig. 6. Insulin absorption.

physiological interpretations, but such considerations are not addressed here. The slow carbohydrates are modeled using a fourth-order compartment model. The fast carbohydrates, however, are modeled with a second-order system representing the very fast absorption occurring when no splitting has to be undertaken. Together they form the total glucose flux:

$$G_{in}(t) = G_{in_{fast}}(t) + G_{in_{slow}}(t). \quad (16)$$

4.2.1. Fast carbohydrates, $G_{in_{fast}}(t)$

Following the discussion above the fast carbohydrates are modeled as:

$$\dot{x}_{fast}(t) = \begin{pmatrix} -c_{11} & 0 \\ c_{21} & -c_{22} \end{pmatrix} \cdot x_{fast}(t) + \begin{pmatrix} 1 \\ 0 \end{pmatrix} \cdot u_{fast}(t), \quad (17)$$

$$G_{in_{fast}}(t) = \begin{pmatrix} 0 & 1/V \end{pmatrix} \cdot x_{fast}(t). \quad (18)$$

The transfer function becomes:

$$H_{in_{fast}}(s) = C_{fast} \cdot (s \cdot I - A_{fast})^{-1} \cdot B_{fast}, \quad (19)$$

$$= \frac{c_{21} \cdot 1/V}{(s + c_{11}) \cdot (s + c_{22})}. \quad (20)$$

Discretization yields

$$x_{k+1}^{fast} = \begin{pmatrix} d_{11} & 0 \\ d_{21} & d_{22} \end{pmatrix} \cdot x_k^{fast} + \begin{pmatrix} b_1 \\ b_2 \end{pmatrix} \cdot u_k^{fast}, \quad (21)$$

$$\Gamma_k^{in_{fast}} = \begin{pmatrix} 0 & 1/V \end{pmatrix} \cdot x_k^{fast}, \quad (22)$$

with the transfer function relationship

$$G_k^{in_{fast}} = C_{fast}(zI - \Phi_{fast})^{-1} \Gamma_{fast} u_k^{fast} = \frac{B_{fast}(z^{-1})}{A_{fast}(z^{-1})} u_k^{fast}. \quad (23)$$

4.2.2. Slow carbohydrates, $G_{in_{slow}}(t)$

The slow carbohydrates were modeled with a fourth order compartment model:

$$\dot{x}_{slow}(t) = \begin{pmatrix} -c_{11} & 0 & 0 & 0 \\ c_{21} & -c_{22} & 0 & 0 \\ 0 & c_{32} & -c_{33} & 0 \\ 0 & 0 & c_{43} & -c_{44} \end{pmatrix} \cdot x_{slow}(t) + \begin{pmatrix} 1 \\ 0 \\ 0 \\ 0 \end{pmatrix} \cdot u_{slow}(t), \quad (24)$$

$$G_{in_{slow}}(t) = \begin{pmatrix} 0 & 0 & 0 & 1/V \end{pmatrix} \cdot x_{slow}(t). \quad (25)$$

The transfer function becomes:

$$H_{slow}(s) = C_{slow} \cdot (s \cdot I - A_{slow})^{-1} \cdot B_{slow}, \quad (26)$$

$$= \frac{c_{21} \cdot c_{32} \cdot c_{43} \cdot 1/V}{(s + c_{11}) \cdot (s + c_{22}) \cdot (s + c_{33}) \cdot (s + c_{44})}. \quad (27)$$

Discretization yields:

$$x_{k+1}^{slow} = \begin{pmatrix} d_{11} & 0 & 0 & 0 \\ d_{21} & d_{22} & 0 & 0 \\ d_{31} & d_{32} & d_{33} & 0 \\ d_{41} & d_{42} & d_{43} & d_{44} \end{pmatrix} \cdot x_k^{slow} + \begin{pmatrix} b_1 \\ b_2 \\ b_3 \\ b_4 \end{pmatrix} \cdot u_k^{slow}, \quad (28)$$

$$\Gamma_k^{in_{slow}} = \begin{pmatrix} 0 & 1/V \end{pmatrix} \cdot x_k^{slow}, \quad (29)$$

with the discrete-time transfer function relationship

$$G_k^{in_{slow}} = C_{slow}(zI - \Phi_{slow})^{-1} \Gamma_{slow} u_k^{slow} = \frac{B_{slow}(z^{-1})}{A_{slow}(z^{-1})} u_k^{slow}. \quad (30)$$

In an oral glucose tolerance test, Dalla Man et al. [27] estimated the glucose absorption rate from the gut. Three different models were fitted to the data corresponding to the fastest carbohydrates here

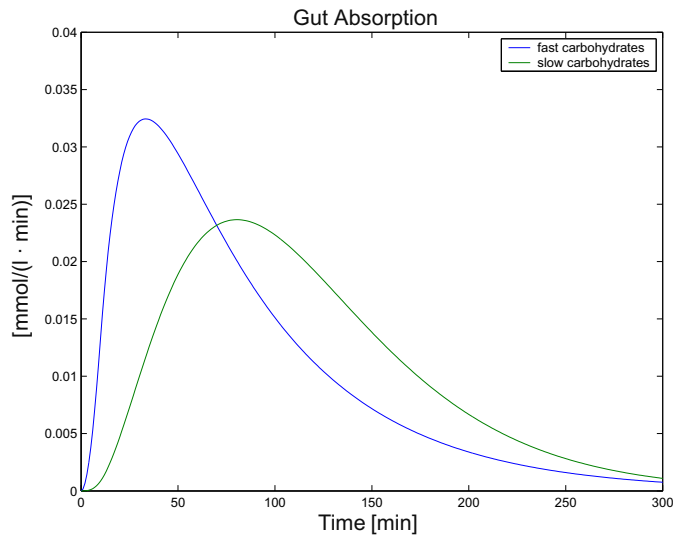


Fig. 7. Gut absorption simulating digestion of 10 g fast and 10 g slow carbohydrates at $t = 0$.

modeled as a second-order compartment model. As no data from the experiment are available, regression cannot be undertaken, but the following dynamical parameters approximately represent the profile; $c_{11} = 0.3$, $c_{22} = 0.9$.

The rate of absorption of a mixed meal peaks at 70–90 min [29]. A normal meal consists of 10–15% fast carbohydrates and 85–90% slow carbohydrates (Appendix A). Bearing this in mind, it seems plausible to argue that the absorption peak for slow carbohydrate absorption peaks at approximately 1.5 h. The following set of parameters gives a plausible absorption profile; $c_{11} = c_{22} = 0.6$ and $c_{33} = c_{44} = 0.5$. To find the parameter c_0 , which determines the gain of the system, the following relation was considered:

$$V \cdot \int_0^{\infty} G_m dt = \eta \cdot C. \quad (31)$$

Here, C is the amount of ingested carbohydrates and η is the efficiency of absorption. This relation states that the sum of absorbed carbohydrates equals the sum of ingested carbohydrates minus the loss in the intestine. According to [27] the absorption efficiency, η is approximately 86%. Using these values, simulation of the digestion of 10 g fast and 10 g of slow carbohydrates resulted in the absorption profiles seen in Fig. 7.

Another way to get a first estimate of the sub-models is to have a closer look at the correlation between the inputs and the blood glucose change. In Fig. 8, the correlation for the slow and fast carbohydrates and the blood glucose rate of change can be seen. The blood glucose rate of change is approximated by a forward difference approximation. Here, the slow carbohydrates seem to act significantly faster than proposed above. The correlation curve for the fast carbohydrates, however, corresponds quite nicely. This may be explained by the fact that the slow carbohydrates are almost always ingested simultaneously with the fast. The fast carbohydrates, which have a significantly higher gain, thus affect the slow carbohydrates correlation curve making it look faster than it really is.

5. Data pre-processing

As result of detrending, the glucose data were reduced by the average over the two weeks. No obvious outliers could be found in the data series.

The interesting question is: Do these measurements contain sufficient information to make a reconstruction of the original

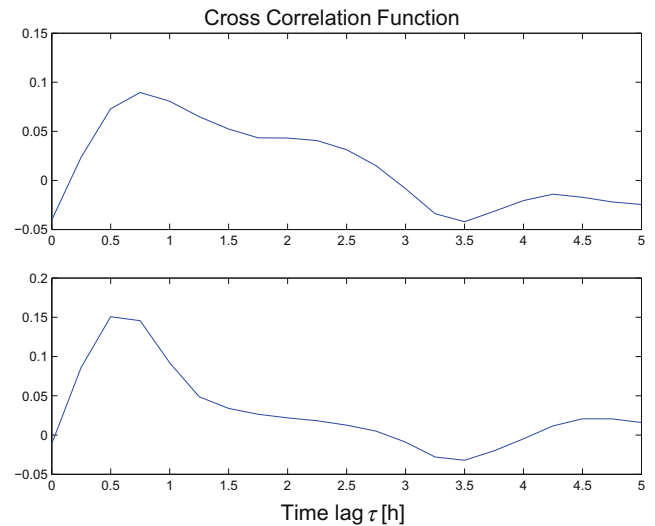


Fig. 8. Cross correlation function between blood glucose change and carbohydrate inputs for slow (upper diagram) and fast (lower diagram) carbohydrate inputs, respectively, vs. time lag τ [h].

signal possible, considering the Shannon sampling theorem $f_s \geq 2f_{max}$ where f_{max} is the highest frequency of interest? And if so, is the proposed method of interpolation an efficient and reliable way to do so? According to [15] at least 8 samples per day are needed to get the lowest essential dynamics of the system, namely the rise and fall of the blood glucose level due to the carbohydrate intake. This relies on the assumption that the meal related period is about 6 h. (Later, this assumption is supported by the periodic behavior of the blood glucose change in Fig. 13.) So sampling every third hour is needed to capture the basic meal related dynamics, but what sampling frequency is needed to reconstruct the blood glucose curve reliably? To find the highest frequency of interest records of 56 patients monitored by MiniMed¹ were analyzed. These data were sampled at 5 min intervals, well below the fastest dynamics of the system. The data were resampled at a lower rate and splined using the reconstructing method used for the home-monitored data. The interpolated home-monitored data have a similar spectral composition as the 120 min resampled MiniMed data, at least for the lower frequencies.

In Fig. 9 a comparison between the original MiniMed data and the resampled and spline-interpolated data of a representative patient can be seen. The patient data used here for visualization of the correspondence between the resampled, interpolated data and the original data incorporate some typical and important features of blood glucose data. Rapid and large fluctuations within the normal range of a diabetic make it suitable as a reference.

In the upper diagrams, the data were resampled to a sampling interval of 30 and 60 min. The interpolated curves follow the MiniMed data without complications, smoothing the noisy original. In the lower diagrams, the interpolated curves have more trouble keeping up with the original. However, most of the larger variations are present in the interpolation and the total impression is that the splined curves follow the original quite well, but for some few quick ups and downs. Glucose self-monitoring does not follow a strict sampling schedule. Rapid changes in the blood glucose are often experienced as hypoglycemia, changes into hypoglycemia or hyperglycemia are often recognized and these circumstances call for unscheduled measurement to establish glycemic status. Therefore, the high and low peaks were represented in the home-moni-

¹ Provided by Medtronic and Novo Nordisk AS <http://www.minimed.com/>.

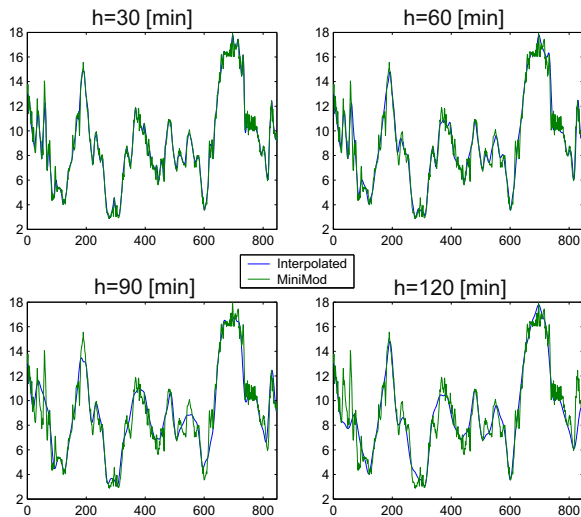


Fig. 9. Comparison between the reconstructed data and the original data for some different resampling frequencies $h = 30, 60, 90, 120$ min for patient number 46.

tored data for most instances, making the reconstruction easier. Assuming that 8 h were spent sleeping a day, the average sampling period becomes about 100 min. Given the above, the interpolated data can perhaps be regarded as having a data reconstruction potential close to the 100 min resampled data. Whereas this signal failed to reproduce some of the fast oscillations, it still made good estimates of the original data. The average RMS between the 100-min signal and the original MiniMed signal was less than 1 mmol/l for the 56 data records considered.

The data were collected in the so-called ‘honeymoon’ period during which the pancreatic β -cells recover somewhat, resulting in temporary remission with considerably varying insulin doses and glycemic response [18,19]. Mathematically, this translates into time-varying model parameters. In order to estimate and validate different models, data segments with constant parameter values are needed. To find such segments, the data were investigated using the Matlab command `segment`, a recursive ARMAX-type linear model [31]. In Fig. 10, the parameter variations over the time period can be seen. A number of more stationary segments can be identified. Among these segments, the last segment is the most interesting because of a number of factors. Firstly, the patient had the disease a sufficiently long time to make up his own regimen, making insulin inputs more varying thereby increasing the excitation from this signal. Secondly, sufficient time had elapsed since diagnosis to make it plausible that the honeymoon period was over. Thirdly, the daily sum of insulin doses was most uniform for this period suggesting as well time-invariant dynamics.

From this data segment, a smaller segment was extracted corresponding to two weeks of data. The first week was used for parameter estimation and the second week for validation. In Fig. 11, the selected period can be seen. According to tests performed by SKUP (Scandinavian evaluation of laboratory equipment for primary health care), the reproducibility of the glucose meter used had a coefficient of variance of 3–6% [1]. With an average of 8.25 mmol/l for the series this corresponds to a standard deviation of less than 0.5 mmol/l.

5.1. Descriptive statistical data analysis

Clearly, data are strongly periodic, a tendency also noted by looking at the autocorrelation for the inputs in Fig. 12. The insulin doses and the slow carbohydrate intake have a 24-h distinct period. The fast carbohydrates, however, do not show such a clear peri-

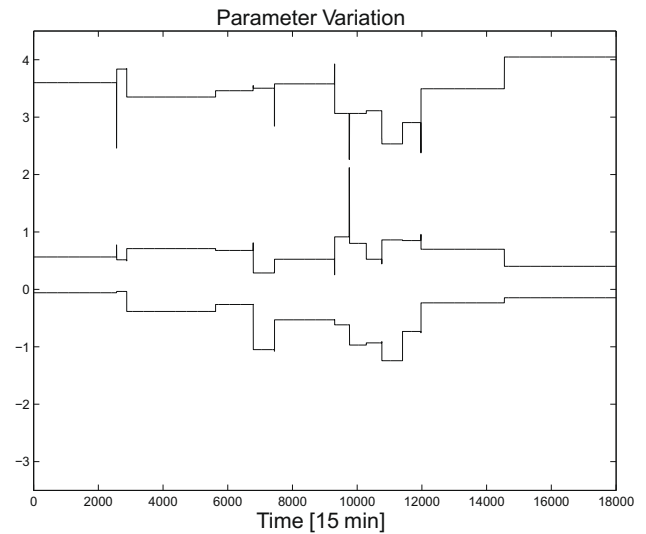


Fig. 10. Data segmentation using Matlab command `segment`. The variation of three (out of 12) parameters.

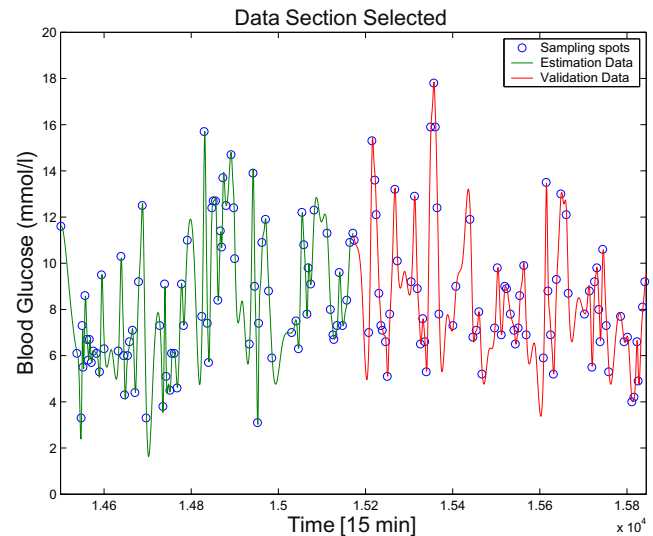


Fig. 11. The data period selected split into data for model estimation (green graph) and for validation (red graph). (For interpretation of the references to color in this figure legend, the reader is referred to the web version of this paper.)

odic behavior, probably due to many snacks at irregular hours. In Fig. 13, the autocorrelation of the blood glucose change can be seen. Here, the 5–6 h periodicity of the glucose flux following a meal referred to by Worthington is quite obvious [15,26].

As seen in Fig. 14, the glucose measurements were not normally distributed. Whereas the samples fluctuated around an average of about 6–8 mmol/l, the deviations were not normally distributed around this mean (Fig. 14), a phenomenon also observed by Carson et al. [33]. Kolmogorov–Smirnov and Bera–Jarque hypothesis tests for normality of logarithmically transformed data were not rejected ($p < 0.05$), thus suggesting a log-normal distribution of blood–glucose data [8, p. 214].

6. Results

The glucose–insulin dynamic system was identified to consist of three different main parts; the glucose subsystem, the insulin subsystem and the glucose–insulin interaction (Fig. 15). Using the lit-

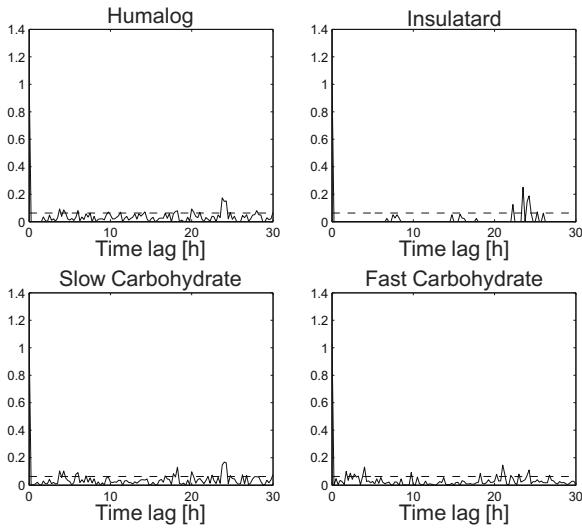


Fig. 12. Autocorrelation functions of inputs: autocorrelation function of Humalog dose (upper left); autocorrelation function of Insulatard dose (upper right); autocorrelation function of slow carbohydrate intake (lower left); and autocorrelation function of fast carbohydrate intake (lower right).

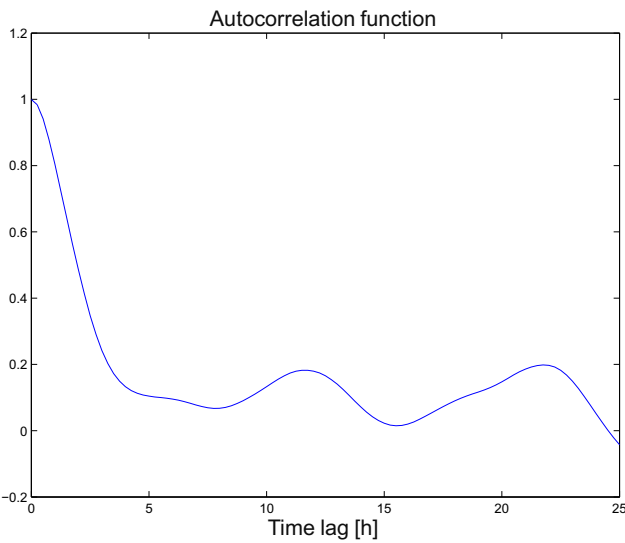


Fig. 13. Autocorrelation function of blood glucose correlation change $\Delta y_k = y_k - y_{k-1}$.

erature based parameter values for the glucose and insulin subsystems the Glucose Insulin Interaction Model (GIIM) was estimated using the estimation data and validated with the validation data. The validation was based on different fitting criteria, such as the AIC, FPE, VAF and residual correlation [8, Chapter 9].

The approach was to firstly investigate linear models. The simplest model with a physiological interpretation is the model proposed by Ackerman et al. [30]:

$$\frac{dG}{dt} = aG(t) + bI(t) + G_{in}(t), \quad (32)$$

$$\frac{dI}{dt} = cG(t) + dI(t) + I_{sub}(t), \quad (33)$$

where $G(t)$ is the blood glucose concentration and $I(t)$ is the plasma insulin level. Additional states can be added, with or without physiological interpretation, thereby the general linear model is given:

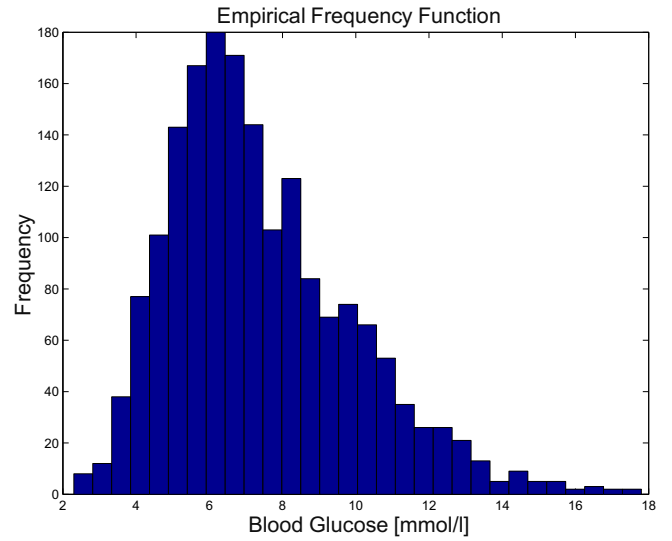


Fig. 14. Empirical frequency functions of blood-glucose sample distribution, apparently with a non-symmetric distribution.

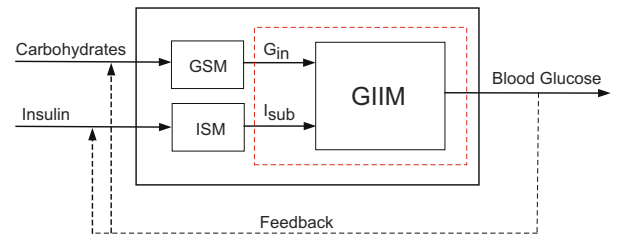


Fig. 15. The partitioning of the system.

$$\dot{x}_{GIIM} = Ax_{GIIM} + Bu, \quad (34)$$

$$y = Cx_{GIIM}, \quad (35)$$

where x_{GIIM} are the different states of the system, and

$$u(t) = (G_{in_{fast}} \quad G_{in_{slow}} \quad I_{sub_{Hum}} \quad I_{sub_{IT}})^T, \quad (36)$$

$$y(t) = G(t). \quad (37)$$

The models investigated were not formulated in the state-space format, however, but used the polynomial representation of the system. Each model was analyzed with respect to Bode diagrams and pole-zero diagrams to investigate possible pole-zero cancellations. The predictive capability of the models was inspected by comparing the 8-step prediction with the splined data, the VAF serving as a comparison tool [22]. The best model according to this criteria is then subject to a nonlinear transformation, using a simple Wiener model. First, however, the ARMA model is reviewed in order to serve as a reference for the other models, giving an indication of the benefit of the use of the sub-models and the different glucose/insulin interaction models.

6.1. ARMA model identification

Previous attempts to predict future blood glucose values given past and present values have previously been reported in [9,10,12]. Postulating an uncorrelated stochastic process $\{e(t)\}$ as input, only previous values of the variable of interest are used for estimation of the ARMA model for the output $\{y(t)\}$ – i.e., $\{y(t)\}$ blood glucose, $\{e(t)\}$ abstract – with

$$A(z^{-1})y(t) = C(z^{-1})e(t). \quad (38)$$

This model may help to get an estimate of the approximate degree of the dynamics. First the AR-model is estimated, and thereafter different orders of the C-polynomial were tested. As can be seen in Fig. 16, all validation criteria yield the same result suggesting sixth-order C-model dynamics. Now, to make the prediction error white the C-polynomial is estimated as well. This yields the following model:

$$A(z^{-1}) = 1 - 3.041z^{-1} + 3.71z^{-2} - 2.238z^{-3} + 0.5845z^{-4} + 0.01778z^{-5} - 0.02505z^{-6} \quad (39)$$

$$C(z^{-1}) = 1 + 0.453z^{-1}. \quad (40)$$

The residual correlation functions in Fig. 17 exhibits close-to-white-noise correlation properties and the one-step-ahead prediction was almost perfect with a fit of 99.97%. In Fig. 18, the 8-step (or 2 h) ahead optimal prediction on the validation data using this model is shown.

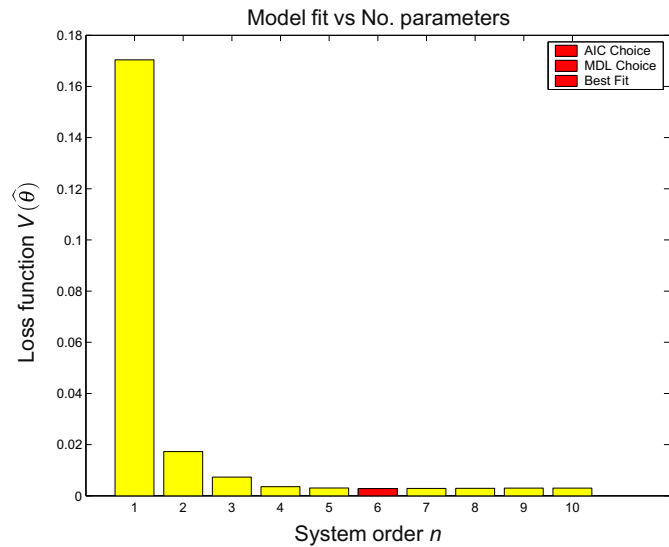


Fig. 16. Model fit of AR model.

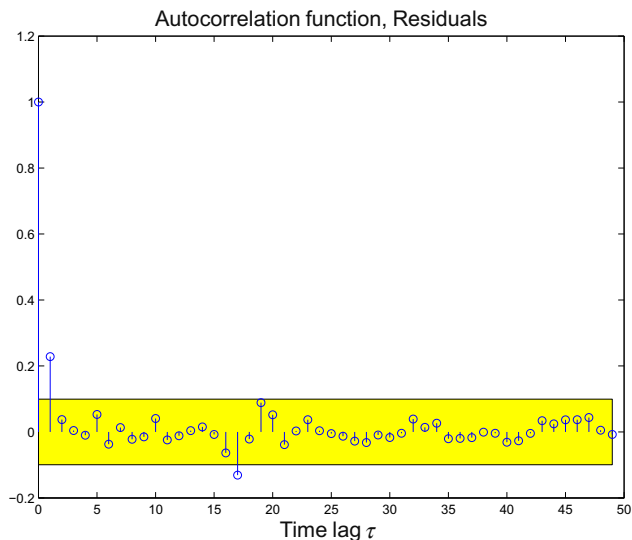


Fig. 17. Residual autocorrelation analysis, ARMA model.

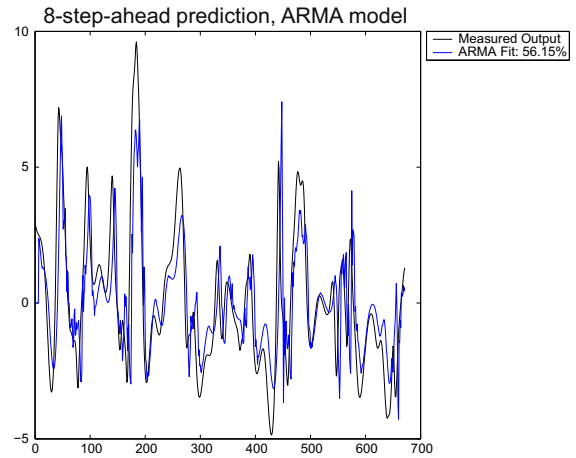


Fig. 18. Blood glucose 8-step-ahead (two-hour-ahead) prediction, ARMA model (blue graph) and measured blood glucose (black graph). (For interpretation of the references to color in this figure legend, the reader is referred to the web version of this paper.)

6.2. Linear models – ARMAX

The ARMAX is a general linear model structure admitting inputs other than white-noise processes. Here, the insulin absorption and the glucose flux were used as inputs

$$A(z^{-1})y(t) = B_1(z^{-1})G_{in}(t) + B_2(z^{-1})I_{sub}(t) + C(z^{-1})e(t).$$

Sets of system orders and time delays were tested according to Table 1. In Table 2, the proposed model structures of the various different validation criteria can be seen. Noteworthy is that the MDL criterion indicates that the inputs did not contribute enough to compensate for the added complexity of the model. Here, the model structure selected by AIC was chosen with residual correlation as seen in Fig. 19. Apparently the residuals were not uncorrelated, and thus a colored noise model had to be estimated. Various different orders of the C-polynomial were tested and evaluated according to best fit, thus yielding the following model:

$$A(z^{-1}) = 1 - 2.817z^{-1} + 3.119z^{-2} - 1.587z^{-3} + 0.1871z^{-4} + 0.1539z^{-5} - 0.04495z^{-6}, \quad (41)$$

$$B_1(z^{-1}) = -0.2095z^{-2}, \quad (42)$$

$$B_2(z^{-1}) = 2.917 - 2.569z^{-1}, \quad (43)$$

$$C(z^{-1}) = 1 + 0.6069z^{-1}. \quad (44)$$

Table 1
ARX model structure investigated.

Parameter	n_A	n_{B_1}	n_{B_2}	k_1	k_2
Range	5–10	0–3	0–3	0–3	0–3

Table 2
ARMAX model structure chosen.

Parameter	Loss	MDL	AIC
n_A	6	6	6
n_{B_1}	2	0	1
n_{B_2}	2	0	2
k_1	0	0	2
k_2	3	0	0

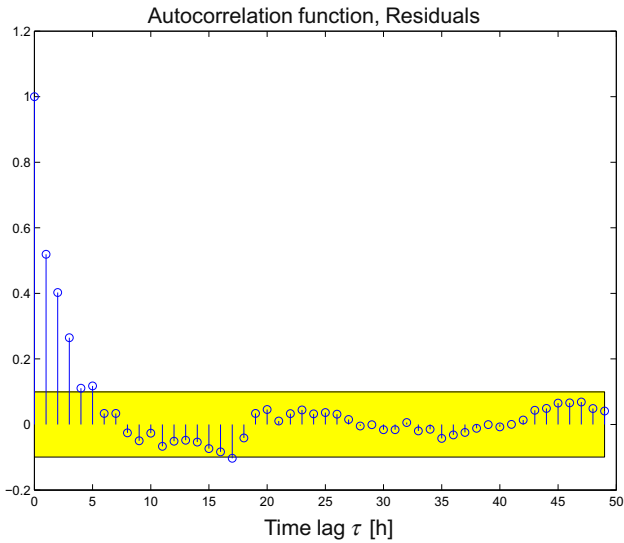


Fig. 19. Residual autocorrelation analysis for ARX model.

The correlation of the residuals may indicate that the noise dynamics differ from the other system dynamics.

6.2.1. Prediction

In Fig. 20, the 8-step-ahead prediction using this model can be seen. The improvement from the ARMA-model is quite small. Different weighting values were tested to investigate whether the model improves when the real measurements were given a higher weight. No improvement was found by weighting the real measurements heavier than the interpolated values.

6.3. Subspace-based model identification

According to the validation criteria, the best model was found for $n=6$ with $s=8$. However, this model was unstable with a pole-pair outside the unit circle. The second best model ($n=4$, $s=6$) was also the model of least complexity. The predictive properties of the subspace-based models were comparable to the ARMAX models. In Fig. 21, the 8-step prediction of the $n=6$, $s=9$

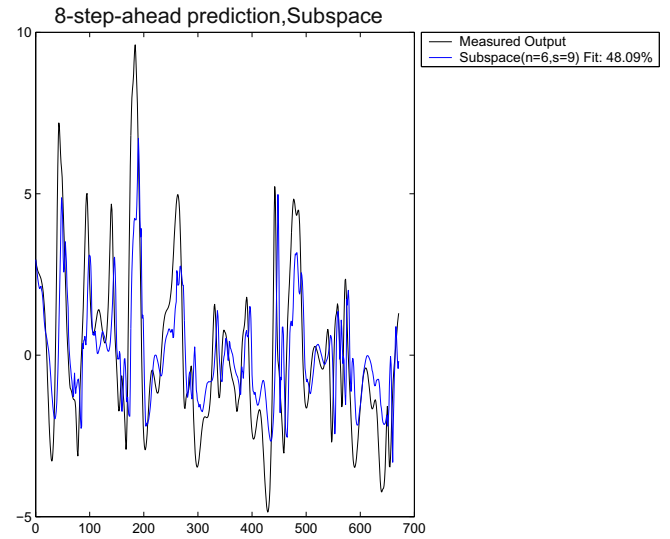


Fig. 21. Blood glucose 8-step-ahead (two-hour-ahead) prediction, Subspace-based model identification (blue graph) and measured blood glucose (black graph). (For interpretation of the references to color in this figure legend, the reader is referred to the web version of this paper.)

can be seen. The VAF was significantly lower than that for the ARMAX model.

6.4. The general transfer function model (GTFM)

Considering the high level of correlation in the residuals in the previous models it may be an idea to consider separating the dynamics in the system. By the general transfer function model the different inputs and the noise model all have different dynamics:

$$A(z^{-1})y(t) = \frac{B_1(z^{-1})}{F_1(z^{-1})} \cdot u_1 + \frac{B_2(z^{-1})}{F_2(z^{-1})} u_2 + \frac{C(z^{-1})}{D(z^{-1})} e(t). \tag{45}$$

The model was estimated for the sets of orders in Table 3. The validation criteria all selected the model structure seen in Table 4. Estimating the parameters gave the model:

$$A(z^{-1}) = 1 - 3.209z^{-1} + 4.257z^{-2} - 2.966z^{-3} + 1.087z^{-4} - 0.1613z^{-5}, \tag{46}$$

$$B_1(z^{-1}) = -0.03211 + 0.01213z^{-1}, \tag{47}$$

$$B_2(z^{-1}) = 0.9626 - 1.414z^{-1} + 0.5386z^{-2}, \tag{48}$$

$$F_1(z^{-1}) = 1 - 0.01277z^{-1} + 0.5702z^{-2} - 0.6425z^{-3}, \tag{49}$$

$$F_2(z^{-1}) = 1 + 0.4967z^{-1} - 0.06102z^{-2}, \tag{50}$$

$$C(z^{-1}) = 1 + 0.4572z^{-1}, \tag{51}$$

$$D(z^{-1}) = 1 + 0.1633z^{-1}, \tag{52}$$

with residuals almost uncorrelated (Fig. 22). As compared to the ARMAX model, the predictive capability somewhat improved (Fig. 23).

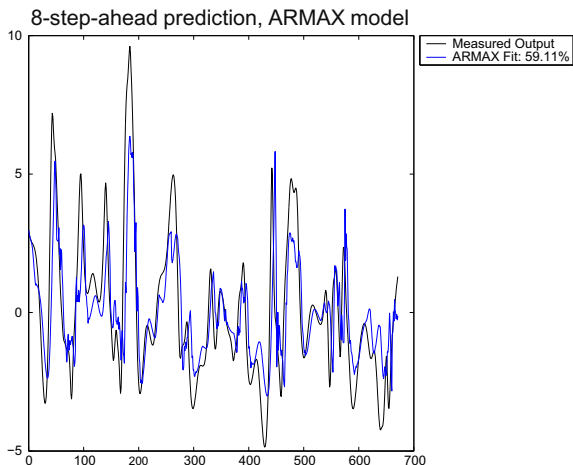


Fig. 20. Blood glucose 8-step-ahead (two-hour-ahead) prediction, ARMAX model (blue graph) and measured blood glucose (black graph) vs. time [15 min]. (For interpretation of the references to color in this figure legend, the reader is referred to the web version of this paper.)

Table 3

Sets of system orders to evaluate for GTFM of Eq. (45).

n_A	n_{B_1}	n_{B_2}	n_{F_1}	n_{F_2}	n_C	n_D	k_1	k_2
3–6	2–3	2–3	2–3	2–3	0–3	0–3	0–2	0–2

Table 4
Chosen model structure, GTFM.

n_A	n_{B_1}	n_{B_2}	n_{F_1}	n_{F_2}	n_C	n_D	k_1	k_2
5	2	3	1	1	3	2	0	0

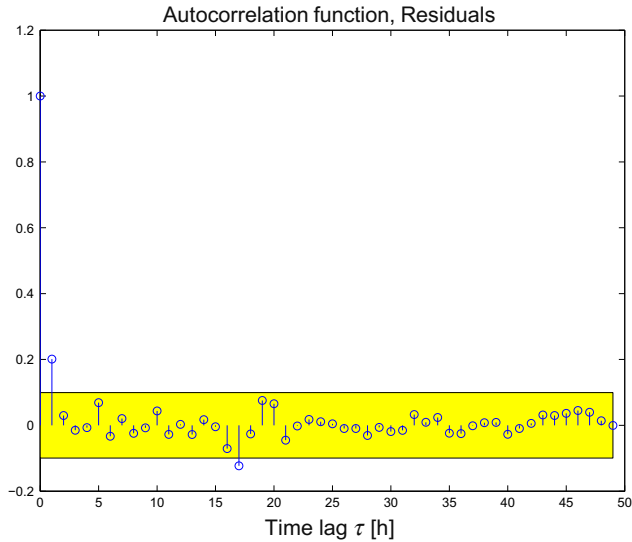


Fig. 22. Residual autocorrelation analysis, general transfer function model of Eq. (45).

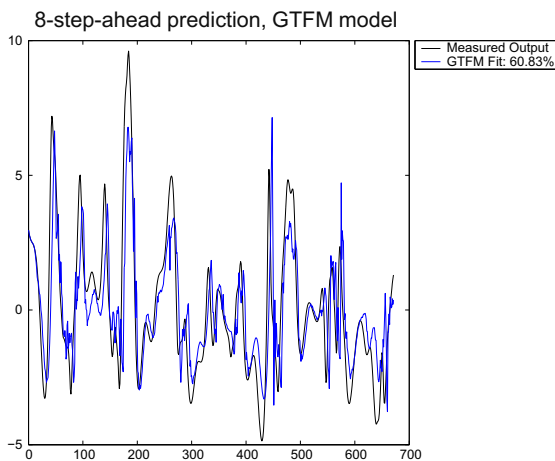


Fig. 23. Blood glucose 8-step-ahead (two-hour-ahead) prediction, General Transfer Function Model (blue graph) and measured blood glucose (black graph) vs. time [15 min]. (For interpretation of the references to color in this figure legend, the reader is referred to the web version of this paper.)

6.5. Nonlinear models

To clarify the linear relationship between the input variables and the blood glucose values the coherence was investigated. In Fig. 24, the plain and windowed coherence plots can be seen. The windowed plots indicate that it may be insufficient to use these inputs to explain the glucose response, possibly caused by factors such as high levels of disturbance affecting the system, non-represented inputs and nonlinearities in the dynamics. Since the linear models proved insufficient to represent the system indicating nonlinear relationships, supported by the coherence plots, nonlinear models must be considered. Here, a number of possible opportunities for making the models nonlinear are investigated. First, the

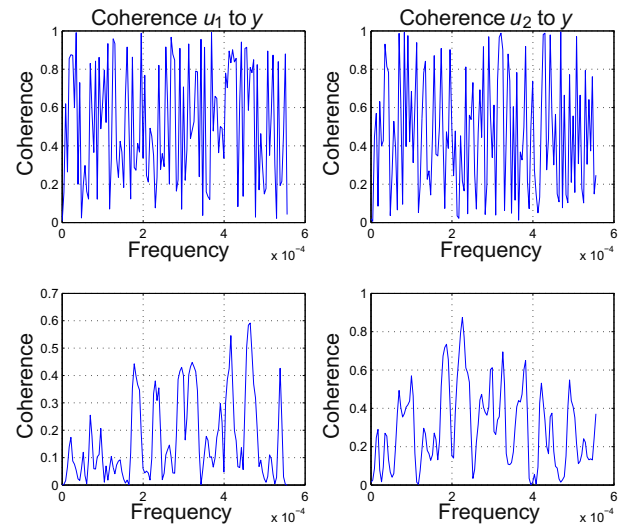


Fig. 24. In the upper graphs, the unwindowed coherence spectra from insulin and glucose inputs to blood glucose output and in the lower graphs coherence spectra using a Hanning window ($L = 128$).

data can be transformed before the linear models were fitted. Two different transformations of the blood glucose data were considered below. Another possibility is the Hammerstein and Wiener models [8]. A Hammerstein model is basically a nonlinear transformation of the inputs thereafter the normal linear models is used. Some simple transformations are considered in the NARMAX section below. The Wiener model consists of making a nonlinear transformation of the output of the linear model. In the GTFM-Wiener model section below, Chebychev polynomials were considered for such a nonlinear function of the output.

6.5.1. Data transformations

Previously, the log-normal character of the blood glucose samples was investigated. A test of log-normality was undertaken, and passed for $p < 0.05$. Thus, a natural nonlinear transformation is to take the natural logarithm of the glucose data

$$y_{\log} = \log(y). \quad (53)$$

This concept was tested for all the models discussed above, but without improvement (Fig. 25). Another transformation proposed by Kovatchev et al. [35] is:

$$y_{kov} = 1.794(\log(y))^{1.026} - 1.861. \quad (54)$$

This transformation was also used in these models, but without further success.

6.5.2. NARMAX

From the coherence diagrams in Fig. 24, there appears to be a poor linear relationship between the inputs and the output. To overcome this it is possible to apart from using the ordinary glucose and insulin inputs take nonlinear transformations of them and use as regressors. Systematically, this is done using for example neural networks or radial basis functions. It is also possible to use other variables which lack obvious physiological explanation as regressors. One such variable is the time of the day. As mentioned in the physiology chapter the dynamics of the system is believed to vary over the day. Basically any variable believed to affect or correlate with the output may be used to try to explain the behavior of the output.

For the models presented above the following simple nonlinear functions were tried to create new inputs:

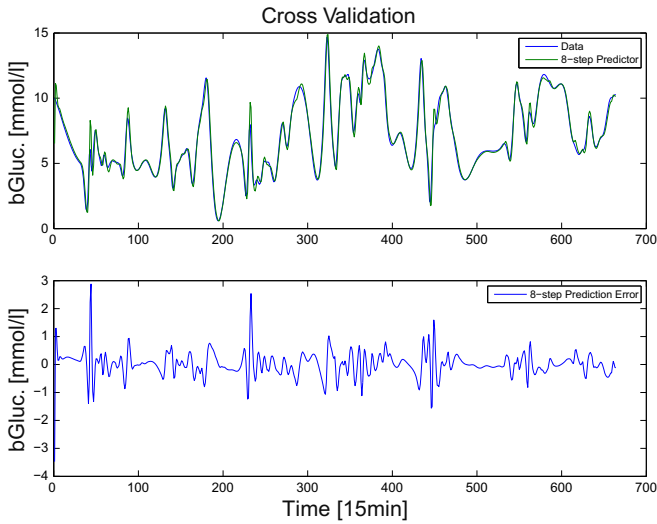


Fig. 25. Cross validation of 8-step-ahead (2 h) prediction based on subspace-based identification using log-normal transformation and Kalman filter with VAF 97% and prediction error $\hat{\sigma}^2 = 0.196$.

$$u_{ij} = u_1^i u_2^j \quad i, j \in \{0, \dots, 3\}. \tag{55}$$

The time of the day was also tried as an input. No significant improvement could be seen.

6.5.3. *GTFM-Wiener*

The linear model can be extended by a nonlinear function on the output. Such a model is called a Wiener model:

$$A(z^{-1})y(t) = \frac{B_1(z^{-1})}{F_1(z^{-1})}u_1 + \frac{B_2(z^{-1})}{F_2(z^{-1})}u_2 + \frac{C(z^{-1})}{D(z^{-1})}e(t), \tag{56}$$

$$y_w(t) = h(y(t)),$$

where $h(y(t))$ is a nonlinear function. Here, Chebychev polynomials were used to represent this function. Polynomials of order 1–25 were tested and evaluated using the Akaike criteria. Using this polynomial, the prediction improved somewhat (Fig. 26).

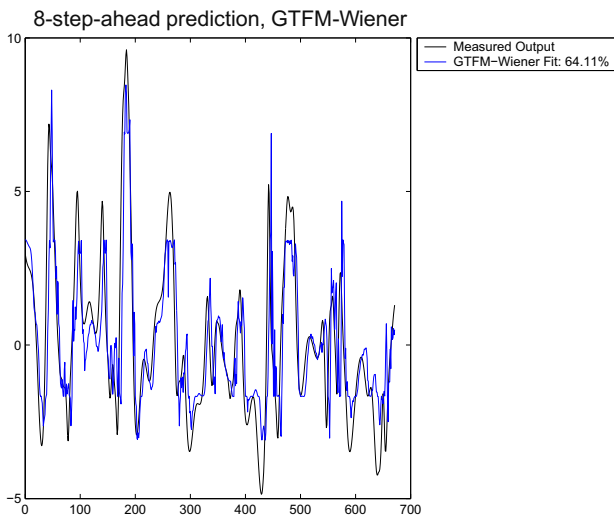


Fig. 26. Blood glucose 8-step-ahead (two-hour-ahead) prediction, GTFM-Wiener model (blue graph) and measured blood glucose (black graph) vs. time [15 min]. (For interpretation of the references to color in this figure legend, the reader is referred to the web version of this paper.)

7. Discussion

The problem of modeling blood–glucose dynamic in diabetes has many difficulties to be discussed below:

The data used in this paper were collected from a newly diagnosed IDDM patient. The fact that only data from one patient was used raised the question of validity for the application of the results in other patients. Many of the problems and properties with the studied system, however, are general and relevant for modeling of other diabetics as well. Data were collected during 6 months in a diabetes diary. The size and timing of each meal sometimes had to be noted afterwards. Many meals, especially snacks are thus not represented correctly. The interpretation and estimates of the food-intake data are somewhat arbitrary. The predefined meals of Appendix A are very coarse estimates and do not span the range of intake sufficiently.

7.1. Interpolation of blood glucose curve

The interpolation routine used may be a poor method to reconstruct the data and thus introduce false dynamics in the time series. The data were sampled at an average of 9.3 samples/day. Assuming that 8 h a day is spent sleeping when no sampling is undertaken, this corresponds to a sampling period of approximately 100 min. These samples were interpolated using a least squares splining method to get a sampling rate of 15 min. The spectrum of the sampled and interpolated signal was compared with the spectrum of an average of patients monitored by Mini-Med, a sampling device collecting samples every fifth minute. The MiniMed samples were also resampled at different rates up to every third hour and interpolated using the same method as for the meter monitored data to get samples every 15 min. The spectra of these new signals were also compared to the interpolated data. The spectrum of the interpolated data falls between the spectra of the signal sampled at 60 min and the signal resampled at every 120 min. These signals were compared to the original signal and evaluated according to their ability to resemble the original signal. The 60-min signal has little trouble following the original signal. On the other hand, the 120-min signal failed to model the most rapid oscillations and has a significantly higher maximum error. The interpolated data had an average sampling rate of every 100 min. The rapid changes in blood glucose concentration were often experienced as hypoglycemia and thus call for sampling to establish glycemic status. Thus, the rapid changes were often captured in these extra, unscheduled samples. More effort is required to analyze optimal sampling schedules and robust and correct interpolation techniques.

7.2. Identifiability issues

The only quantity of the system accessible to measurements is the blood glucose concentration. Glucose flux from the absorption of meals and the insulin absorption from the subcutaneous depots are not available for measurements. This constitutes a significant difficulty in the estimation of the sub-models and their output impact on the GIIM. The absorption of rapid-acting insulin and the glucose flux from carbohydrate intake are almost always present at the same time, making it difficult to access the influence of each input. This problem is difficult to avoid, since separating the insulin injections and carbohydrate intake may create unacceptable risks for the patient. This is undoubtedly one of the major problems in efforts to model and estimate the system under these conditions. The only possibility to get reliable estimates of these sub-models is to conduct clinical experiments such as glucose clamp techniques or tracer methods. Such experiments are cumbersome and not appropriate for routinely use.

7.3. The sub-models

The energy intake was considered to consist solely of slow and fast carbohydrates. As food contains two other major sources of energy (i.e., fat and protein), this assumption is not true. Metabolic conversion of fat and proteins into glucose and free fatty acids (FFAs) may take place in the liver in the post-absorptive stage. Therefore, fat and proteins also have an impact on the metabolism of the body with direct and indirect influence on the GIIM. Regarding carbohydrates there is a vast spectrum of various different mono-, di- and polysaccharides and to simply division their absorption dynamics in two categories is probably an oversimplification.

The fast carbohydrates were modeled using a second-order compartment model. Looking at the absorption profile from [27], this seems to be a plausible model to represent the absorption. The slow carbohydrates were modeled using a fourth-order compartment model. Slow carbohydrates first have to be digested into glucose before absorption and therefore have a delay between intake and absorption. The fourth-order compartment model creates such a delay in the absorption. As mentioned above, fat and protein have not been regarded. Apart from providing energy they influence the absorption dynamics.

The GSM used in this paper was kept very simple for a number of reasons. Firstly, this paper deals with the entire glycemic system and a thorough modeling would simply take too much effort. Secondly, the information about the contents of the meals is rather scarce in the diabetes diary. Meals are simply noted as breakfast, lunch, dinner and an estimate of their size; small, normal or large. Thirdly, the accuracy in the model has to stand in proportion to the accuracy of the inputs. Notes on the exact amounts of carbohydrates, protein and fat in the diary is simply not realistic.

Whether these simple models are too simplified to describe the absorption in an acceptable way remains to be investigated. Most likely research has to be targeted at physiological modeling and understanding of how the digestive and absorptive processes are influenced by the composition of the meals. However, it has to be borne in mind that the data available cannot be assumed to be very accurate. For this effort also has to be put on developing simple and accurate ways to estimate the content of a meal. In Australia, food producers can now have their products measured with the glycemic index analysis and labelled with the glycemic index on the package. Thereby, the consumers can easily get an estimate of the glycemic effect of the product. Glycemic Index is a debated issue, and it has some serious shortcomings in describing the absorption profile of meal – for reviews of glycemic index and its usage, see [29,36–40,26].

The ISM was modeled using a second-order compartment model for the rapid-acting insulin and the Berger model for the slow-acting insulin [24]. The rapid-acting insulin had a very fast onset, which the second-order model is able to represent. The dynamics of the slow-acting insulin is widely considered to be dose-dependent, fact which makes linear compartment models unsuitable. Instead, the Berger model was used to represent the dynamics. The nonlinear nature of the Berger model makes it difficult to estimate and therefore parameter values found in the literature were used. This is of course not optimal since these average parameter values likely differ from those representing this specific patient. The absorption of the slow-acting insulin, however, is slow making it less sensitive to interpatient variations. As previously mentioned, there are large interpersonal variations in the submodels between different subjects. In this paper mean population parameter values from the literature have been used. Individualized parametrization requires cumbersome clamp or tracer experiments, and therefore has not been addressed here [34]. Non-individualized parameters constitute a severe limitation for the prediction and undoubtedly

'deteriorate' or 'depreciate' the result. Additionally, there is a considerable interpersonal variability in the absorption of insulin due to injection site, depth of the deposition and variations in peripheral turn-over rate. Variation in glucose absorption can be expected as well, an uncertainty that cannot be modeled at all, thereby limiting the prediction capacity unless it somehow can be retrieved in an on-line setting.

7.4. Unrepresented inputs

The modeling was based on measurements and estimates of blood glucose, size and timing of insulin injection doses and meals. However, there may be other inputs with important influences on the dynamics of the system. One such input may be physical exercise. Apart from having blood glucose lowering effect due to the utilization of glucose in the muscle cells, exercise also has a positive effect on insulin sensitivity. Thus, the effect of insulin is also enhanced. This variable was not considered mainly due to difficulties in quantifying it properly. Another variable of interest is the time of the day. The dynamics of the system is believed to vary over the day, especially in the morning as compared to the rest of the day. In this paper this variable has simply been tried as a regressor, but without much success. An alternative would be to divide the day in different segments and with multiple sets of parameters, one set for each segment. Finally, alcohol intake also has to be considered as a specific input. The metabolism of alcohol disturbs the endogenous glucose production, and thus has a glucose lowering effect. This variable was not been considered, mainly due to that such consumption has not been noted in the diary.

7.5. The linear models of GIIM

In Figs. 27 and 28, a comparison between the Bode diagrams of the previous models can be seen. The transfer functions fall into two separate categories – i.e., the subspace-based models, the ARMAX and the GTFM models. The subspace-based models put more emphasis at the higher frequencies, while the ARMAX and GTFM have a typical low pass performance. Since these models have the best predictive capability, they probably also best resemble the true system. Therefore, focus will be on these two models. There are some important differences between the models. There is a resonance peak in the insulin/GIIM transfer function in the

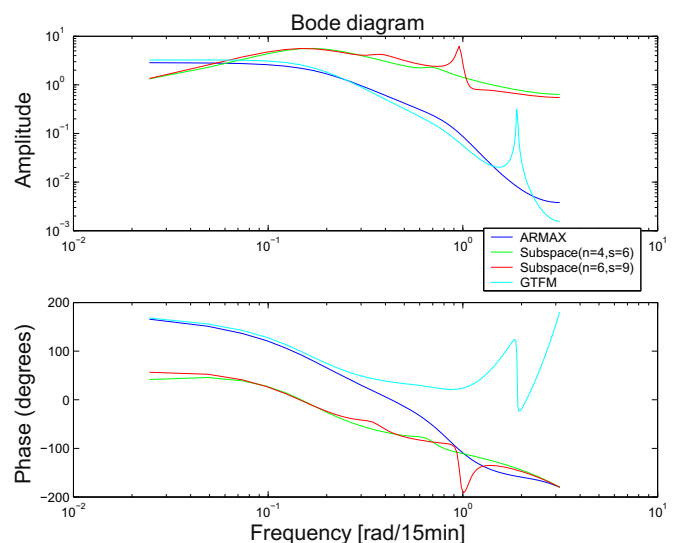


Fig. 27. Comparison Bode diagrams, ISM/GIIM to blood glucose for various identification methods.

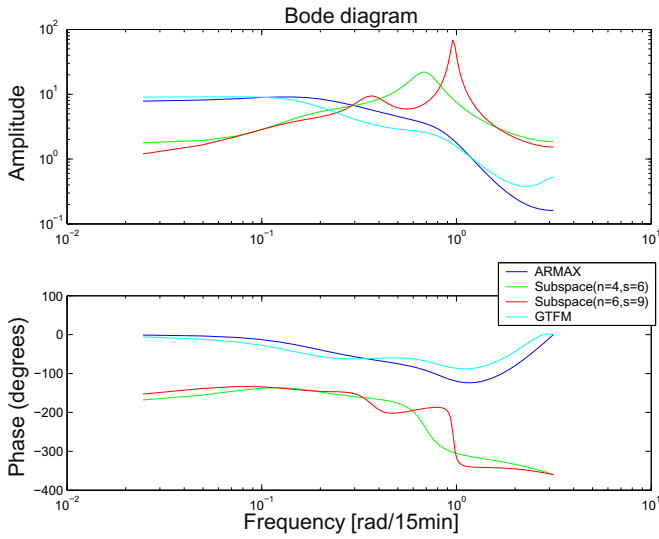


Fig. 28. Comparison Bode diagrams. GSM/GIIM to blood glucose for various identification methods.

GTFM not present in the ARMAX model. Another difference is the noise dynamics. In the ARMAX model, the residuals are still correlated, while in the GTFM they are practically uncorrelated. This may in part be explained by the GTFMs general better ability to explain the system using the inputs, but also by having a slightly different noise model as can be seen in Fig. 29. In all the models of the insulin/GIIM dynamics the pole pair close to the real one is present. Likewise all models agreed that the glucose/GIIM transfer function has a pole pair somewhere in the vicinity of $0.5-0.6 \pm (0.5-0.8)i$. This may indicate that these dynamics are essential parts of the system. The best model according to VAF for the 8-step-ahead prediction is the GTFM. In Fig. 30, the models prediction error standard deviation can be seen for predictions between 1 and 10 steps forward. Whereas the GTFM was the best model in the whole range, the result was not undisputed; the best linear model is obviously not capable of describing the system very well. As seen in Figs. 30 and 31, the predictive capacity degraded very fast as the prediction horizon increased. Already with four-step-ahead (1 h) prediction, the model had difficulties with under- and overshoots.

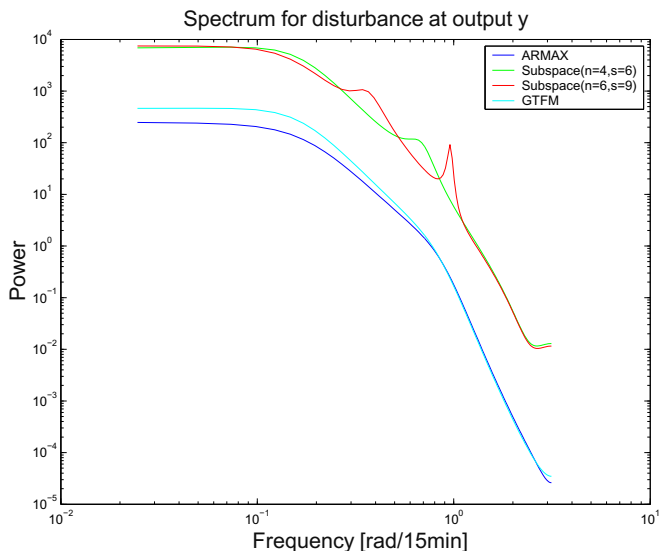


Fig. 29. Bode diagram. Noise dynamics for various identification methods.

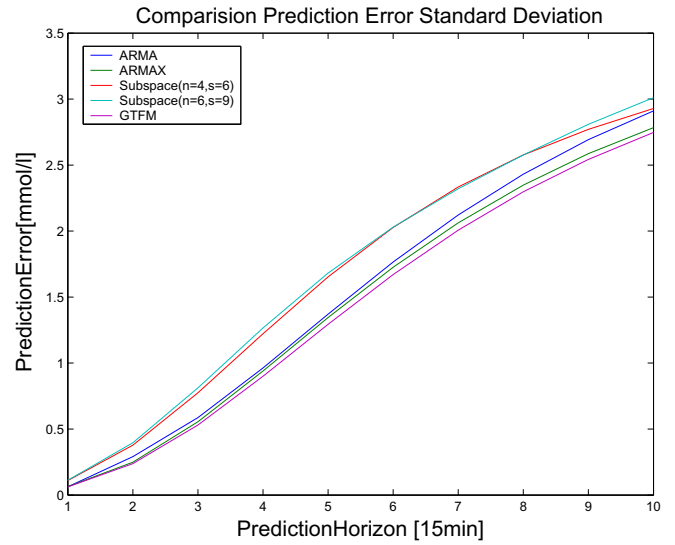


Fig. 30. The prediction standard deviation vs. prediction horizon [15 min].

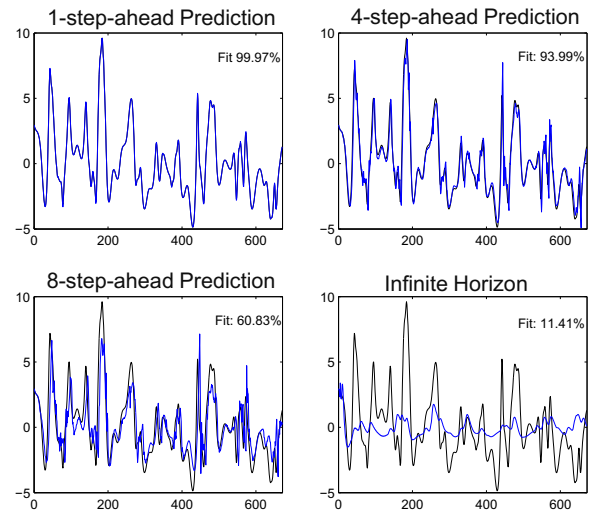


Fig. 31. Illustration of the degradation of predictive capacity, GTFM, for various prediction horizons: $\tau = 1$ (upper left); $\tau = 4$ (upper right); $\tau = 8$ (lower left); $\tau = \infty$ (lower right).

After 8 steps these prediction problems escalated, making the predictions rather poor. In the last diagram the pure simulation ($\tau = \infty$) can be seen. In Fig. 32, the simulation can be seen clearer. In the upper diagram, the simulated data and the splined data can be seen again. The model had obvious problems with the magnitude. In the lower diagram, the output of the model was simply scaled with a factor of 2.5. In Fig. 33 the system was simulated using varied inputs; $u_{i,sim} = (1 \pm 0.25)u_i$. This is supposed to represent the natural uncertainty in the absorption processes.

Judged from the target objective of two-hour-ahead prediction with a prediction error smaller than 1 mmol/l in 95% of the cases, the 8-step prediction accuracy was insufficient for all the models. The models had difficulty with the high peaks and the low bottoms of the data. Whereas this is probably an artefact of nonlinearities in the system, it could also be an effect of underestimated GIIM gains due to correlated inputs with cancelling effects. This problem can be seen even clearer in the simulation of the GTFM. By simply scaling the output, the simulated output resembles the true data at

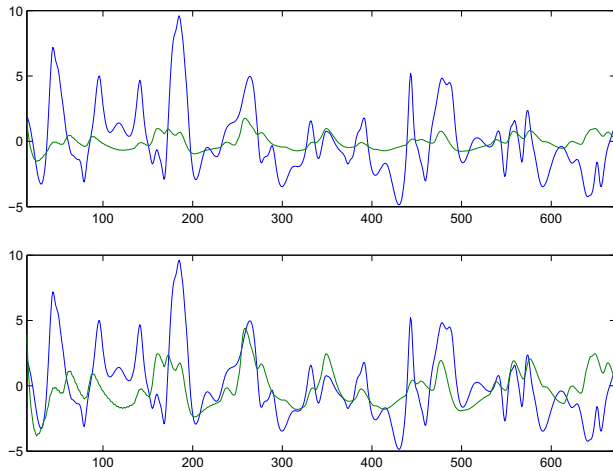


Fig. 32. Simulated model (GTFM) output (green) and real data (blue) vs. time (upper diagram). Scaled simulated data and real data vs. time (lower diagram). (For interpretation of the references to color in this figure legend, the reader is referred to the web version of this paper.)

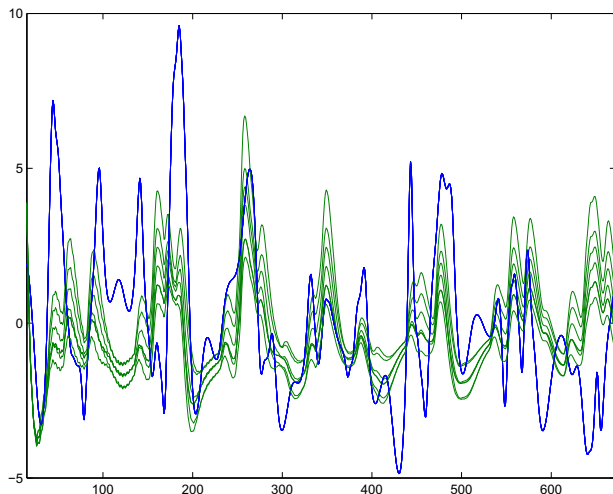


Fig. 33. Simulated data using inputs varied $\pm 25\%$.

some periods. In other segments of the data the model is completely out of track.

Looking at the coherence spectra between the insulin and glucose input to the GIIM and the glucose output, there appears to be a poor linear relationship among these variables. This may in part be explained by that there are unrepresented inputs that have a significant impact on the glucose concentration. Even so, linear modeling would expect higher coherence for the relationship of GSM/GIIM and ISM/GIIM, as these two variables undoubtedly are the most important inputs.

A simple way to make the system nonlinear is to transform the data. In the data chapter the log-normal nature of the blood glucose samples was reviewed and the log-normality hypothesis was not rejected ($p < 0.05$). Therefore, a natural transformation would be to take the natural logarithm of the data. This transform and the transform suggested by Kovatchev et al. [35] were tested on the linear model without improvement. The coherence diagrams did not improve either. Instead some simple Hammerstein and Wiener models were considered to extend the GTFM. The Hammerstein models used did not improve the model performance. Using a Wiener model with a Chebychev polynomial non-linearity, the prediction accuracy improved somewhat.

7.6. Time-varying dynamics

As discussed above, the blood–glucose dynamics vary not only over the time of the day, but also over a longer time span. In Fig. 10, the parameter values of the Matlab algorithm *segment* can be seen with *segment* estimating a recursive ARMAX model for the entire data period. In the diagram, the variation of these parameters over the period can be seen. At onset, the parameters fluctuated very much and then stabilized in the end. The fact that the parameters seem to stabilize may indicate the end of the honeymoon period. The variations in the system dynamics are normally not as rapid and violent as in this data, but there are variations due to continuous β -cell destruction, variations in body mass, level of physical activity, etc. Therefore, it is important to remember that no model is valid forever, but models have to be re-estimated to correspond to the time-varying dynamics.

7.7. Two-hour-ahead predictors

Whereas the best two-hour-ahead cross-validated predictors were found by means of subspace-based identification (Fig. 25) and Wiener-model identification (Fig. 26), the prediction did not uniformly meet our accuracy target of 0.5 mmol/l in transients (Fig. 25). Whereas the two-hour-ahead prediction error standard deviation $\hat{\sigma} = 0.44$ is within the target limits, there are transient events with prediction error of larger magnitude.

8. Conclusions

The purpose of this paper was to develop and evaluate different models of IDDM blood glucose fluctuations, based on one patient's data. The aim was to be able to predict blood glucose values 2 h ahead with a prediction error smaller than 1 mmol/l in 95% of the cases. Whereas the best models – i.e., the log-normalized linear model based on subspace-based identification and the GTFM-Wiener model – did not quite meet our accuracy target of 0.5 mmol/l, the predictor of Fig. 25 is conservative in prediction both of hypoglycemia and hyperglycemia. There are several reasons for the accuracy problems:

- The number of measurements may be too few and the interpolation method not optimal, resulting in a poor reconstruction of the blood glucose curve.
- The system was hard to identify using these data. The inputs act simultaneously, making it difficult to estimate the sub-models and to extract the specific impact of each input on the output. For accurate identification of the insulin and glucose dynamics, it would be desirable to have an experiment design with decorrelated insulin and glucose intakes.
- The system is nonlinear and can thus not be represented by the linear models.
- The sub-models used to describe the glucose flux and the insulin absorption were probably too simple or irrelevant to accurately describe these processes.
- The diary estimates of the size and timing of the meals and insulin injections were not sufficiently accurate.
- Unrepresented variables are probably relevant to describe the system – e.g., physical activity and alcohol intake.

Apart from these difficulties, some other interesting properties of the system are:

- The system dynamics are time-varying especially during the 'honeymoon' phase [18,19].

- The glucose measurements are log-normally distributed.
- All the linear models had some common dynamics. This may indicate that these dynamics are essential to the system.

Whereas this paper did not meet the goals set, it hopefully revealed some interesting features and some of the inherent difficulties of modeling this system. Much effort has to be put at analyzing these issues. A brief survey of possible further research can be found next:

- *Optimal sampling schedule:* Blood glucose sampling conducted with a glucose meter is costly and constitutes a annoyance for the patients. For these reasons the sampling has to be effective. Thus, one research object is to evaluate how many samples, and when these are to be taken, to be able to reliably reconstruct the blood glucose curve.
- *Reconstructing the blood glucose curve:* Given these samples, an effective interpolation algorithm has to be available to reconstruct the blood glucose curve.
- *Modeling the subsystems:* As seen in this paper the sub-models are very important to accurately describe the system. Flaws in the sub-models cannot be corrected in the GIIM. Especially, the GSM is difficult to model, and it must be analyzed with regards to the influence of fat, protein and fiber on the dynamics of the digestive and absorptive processes.
- *Hammerstein–Wiener models using EKF:* The system is nonlinear, and thus calls for nonlinear models. One such concept that may be tested is the Hammerstein–Wiener approach, identified using the extended Kalman filter [41].
- *Physiological modeling:* For a deeper understanding of the dynamics, parameter sensitivity and selection of physiological variables to measure, a physiological model is indispensable [3–5].
- *Exercise:* Exercise probably has an important effect on the dynamics of the system, directly in terms of disposal of glucose, but also indirectly through the effects on the insulin sensitivity.
- *Time-varying dynamics:* The time variations over the elapse of the day has to be considered carefully. If the dynamics shift over the day, different parameter sets of the model have to be considered, one for each segment of the day, for which the parameters can be considered fixed.

Acknowledgments

The first author would like to express his gratitude towards his three supervisors Rolf Johansson, Christian Liisberg and Mona Landin-Olsson for their guidance and many helpful discussions. We would also like to thank Per Hagander at the Department of Automatic Control, Lund University, for his interest and help in providing contacts and Jette Randløv and Jon Hansen at Novo Nordisk AS for literature suggestions and valuable comments on the preliminary manuscript. We are also grateful to Novo Nordisk for providing the MiniMed data and for financial support.

As continuation, the DIAAdvisor™ project within the European FP7-ICT program will pursue research on prediction and predictive control of blood glucose concentration.

Appendix A. Predefined meals

In the diary the meals were noted using the semantic expressions small, normal and large. Below follows a definition of these standard meals in terms of fast and slow carbohydrate content. These definitions have been based on the patient's estimate of the amount ingested, the weighing of some groceries and by the use of [17].

Food	Fast (g)	Slow (g)	Total (g)
Breakfast, normal	10	45	55
Breakfast, small	10	25	35
Lunch, small	5	40	45
Lunch, normal	5	85	90
Dinner, normal	5	85	90
Dinner, large	10	120	130
Snack, small	0	10	10
Snack, normal	0	20	20
Dextrosol, 1 piece	3.5	0	3.5
Sweets, 10 g	8	0	8
Apple	3	20	23
Pear	3	12	15
Banana	11	18	29
Peach	1	9	10
Potato chips, 100 g	0	47	47

Appendix B. List of symbols and abbreviations

B.1. List of abbreviations

Abbreviation	Description
AIC	Akaike information criteria
ARX	Auto regressive with external input
ARMAX	Auto regressive moving average external input
FPE	Final prediction error
GIIM	Glucose/insulin interaction model
GSM	Glucose sub-model
GTFM	General transfer function model
IDDM	Insulin-dependent diabetes mellitus
IDT	Insulin-dependent tissue
IIT	Insulin-independent tissue
ISM	Insulin sub-model
NARMAX	Nonlinear auto regressive moving average with external input
RMS	Root mean square
VAF	Variance accounted for

Symbol	Description	Units
<i>Greek letters</i>		
η	Absorption efficiency	(–)
Γ_{fast}	Γ -matrix of the disc. Fast carb compartment model	(–)
Γ_{Hum}	Γ -matrix of the disc. Humalog compartment model	(–)
Γ_{slow}	Γ -matrix of the disc. Slow carb compartment model	(–)
Φ_{fast}	Φ -matrix of the disc. Fast carb compartment model	(–)
Φ_{Hum}	Φ -matrix of the disc. Humalog compartment model	(–)
Φ_{slow}	Φ -matrix of the disc. Slow carb compartment model	(–)
<i>Roman letters</i>		
a	Constant in the Ackerman model	(min ⁻¹)

Symbol	Description	Units
a_{50}	Constant in the Berger model	(min/U)
A	A -matrix of the extended Ackerman model	(–)
$A(z^{-1})$	Output polynomial in ARMAX, etc.	(–)
$A_{fast}(z^{-1})$	Denominator of the fast carbohydrate compartment model's tf	(–)
$A_{Hum}(z^{-1})$	Denominator of the Humalog compartment model's tf	(–)
$A_{slow}(z^{-1})$	Denominator of the slow carbohydrate compartment model's tf	(–)
$A(t)$	Amount (%) insulin remaining in depot at time t	(–)
A_{fast}	A -matrix of the fast carbohydrate compartment model	(–)
A_{Hum}	A -matrix of the Humalog compartment model	(–)
A_{slow}	A -matrix of the slow carbohydrate compartment model	(–)
b	Constant in the Ackerman model	(mmol U ⁻¹ min ⁻¹)
b_{50}	Constant in the Berger model	(min/U)
B	B -matrix of the extended Ackerman model	(–)
$B(z^{-1})$	Input is polynomial in ARMAX, etc.	(–)
$B_{fast}(z^{-1})$	Numerator of the fast carbohydrate compartment model's tf	(–)
$B_{Hum}(z^{-1})$	Numerator of the Humalog compartment model's tf	(–)
$B_{slow}(z^{-1})$	Numerator of the slow carbohydrate compartment model's tf	(–)
B_{fast}	B -matrix in the fast carbohydrate compartment model	(–)
B_{Hum}	B -matrix in the Humalog compartment model	(–)
B_{slow}	B -matrix in the slow carbohydrate compartment model	(–)
c	Constant in Ackerman model	(mmol ⁻¹ U min ⁻¹)
c_0	Artificial rate coefficient in compartment model	(–)
c_{ij}	Rate coefficient in compartment model to compartment i from j	(–)
C	C -matrix of the extended Ackerman model	(–)
$C(z^{-1})$	Noise polynomial in ARMAX, etc.	(–)
C_{fast}	C -matrix of the fast carbohydrate compartment model	(–)
C_{Hum}	C -matrix of the Humalog compartment model	(–)
C_{slow}	C -matrix of the slow carbohydrate compartment model	(–)
d	Constant in Ackerman model	(min ⁻¹)
d_{ij}	Rate coefficient in discrete compartment model, to compartment i from j	(–)
D	D -matrix of the extended Ackerman model	(–)
$D(z^{-1})$	Noise polynomial in GTFM	(–)
e_k	White noise	(mmol/l)
f_{max}	Maximum frequency of interest	(Hz)
f_s	Sampling frequency	(Hz)

Symbol	Description	Units
$F(z^{-1})$	Input is polynomial in GTFM	(–)
$C_{fast,k}$	Amount of ingested fast carbohydrates at t_k	(g)
$C_{slow,k}$	Amount of ingested slow carbohydrates at t_k	(g)
$D_{Hum,k}$	Amount of injected Humalog at t_k	(U)
$D_{IT,k}$	Amount of injected Humalog at t_k	(U)
$f_{subIT}(t)$	Berger function of insulin absorption	(I ⁻¹)
$G_{in}(t)$	Total Glucose flux	(mmol/l)
$G_{infast}(t)$	Fast carbohydrate glucose flux	(mmol/l)
$G_{inslow}(t)$	Slow carbohydrate glucose flux	(mmol/l)
H_{infast}	Controlled transfer function, fast carbohydrate	(–)
H_{inslow}	Controlled transfer function, slow carbohydrate	(–)
H_{subHum}	Controlled transfer function, Humalog	(–)
$I_{sub}(t)$	Total insulin absorption	(uU/l)
$I_{subHum}(t)$	Humalog insulin absorption	(uU/l)
$I_{subIT}(t)$	Insulatard insulin absorption	(uU/l)
$u_{fast}(t)$	Fast carbohydrate intake	(g)
$u_{Hum}(t)$	Humalog injections	(U)
$u_{IT}(t)$	Insulatard injections	(U)
$u_{slow}(t)$	Slow carbohydrate intake	(g)
s	Factor in the Berger model	(–)
T_{50}	Absorption halftime	(min)
u_1	Another notation for I_{sub}	(uU/l)
u_2	Another notation for G_{in}	(mmol/l)
V	Sum of squared residuals	((mmol/l) ²)
V	The plasma volume	(l)
$x_{fast}(t)$	State vector of the fast carbohydrate compartment model	(–)
$x_{GIIM}(t)$	State vector of the GIIM used in the PEM-identification	(–)
$x_{Hum}(t)$	State vector of the Humalog compartment model	(–)
$x_{slow}(t)$	State vector of the slow carbohydrate compartment model	(–)
$y(t)$	Detrended blood glucose concentration	(mmol/l)
$y_{log}(t)$	$y(t)$ transformed by the natural logarithm	(–)
$y_{kov}(t)$	$y(t)$ transformed by the transform proposed by Kovatchev	(–)

References

- [1] SKUP/2005/43. ACCU-CHEK Compact Plus. A meter designed for glucose self-measurement manufactured by Roche Diagnostics, www.SKUP.nu.
- [2] G.-J. Biessels, Cerebral complications of diabetes: clinical findings and pathogenetic mechanisms, *Neth. J. Med.* 54 (1999) 35.
- [3] R. Bergman, C. Cobelli, Minimal modeling, partition analysis, and the estimation of insulin sensitivity, *Fed. Proc.* 39 (1) (1980) 110.
- [4] C. Cobelli, A. Mari, Validation of mathematical models of complex endocrine-metabolic systems. A case study on a model of glucose regulation, *Med. Biol. Eng. Comput.* 21 (1983) 390.
- [5] C. Cobelli, G. Nucci, S.D. Prato, A physiological simulation model of the glucose-insulin system, in: *Proceedings of the first joint BMES/EMBS Conference, 1999*, p. 999.
- [6] G. Nucci, C. Cobelli, Models of subcutaneous insulin kinetics. A critical review, *Comput. Methods Programs Biomed.* 62 (2000) 249.
- [7] F. Kajiyi, S. Kodama, H. Abe (Eds.), *Compartmental Analysis: Medical Applications and Theoretical Background*, Karger, Basel, 1984.

- [8] R. Johansson, *System Modeling and Identification*, Prentice-Hall, Englewood Cliffs, NJ, 1993.
- [9] T. Bremer, D. Gough, Is blood glucose predictable from previous values? A solicitation for data, *Diabetes* 48 (1999) 445.
- [10] R. Bellazzi, P. Magni, G.D. Nicolao, Bayesian analysis of blood glucose time series from diabetes home monitoring, *IEEE Trans. Biomed. Eng.* 47 (7) (2000) 971.
- [11] F. Ståhl, *Diabetes mellitus modelling based on blood glucose measurements*, Master Thesis TFRT-5703, Department of Automatic Control, Lund University, Sweden, April 2003.
- [12] G. Sparacino, F. Zanderigo, S. Corazza, A. Maran, A. Facchinetti, C. Cobelli, Glucose concentration can be predicted ahead in time from continuous glucose monitoring sensor time-series, *IEEE Trans. Biomed. Eng.* 54 (5) (2007) 931.
- [13] P. Dua, F.J. Doyle III, E.N. Pistikopoulos, Model-based blood glucose control for type 1 diabetes via parametric programming, *IEEE Trans. Biomed. Eng.* 53 (8) (2006) 1478.
- [14] D.J. Cox, L. Gonder-Frederick, L. Ritterband, W. Clarke, B.P. Kovatchev, Prediction of severe glycemia, *Diabetes Care* 30 (6) (2007) 1370.
- [15] D.R.L. Worthington, The use of models in the self-management of insulin-dependent diabetes mellitus, *Comput. Methods Programs Biomed.* 32 (1990) 233.
- [16] R. Bellazzi, C. Siviero, M. Stefanelli, G. Nicolao, Adaptive controllers for intelligent monitoring, *Artif. Intell. Med.* 7 (1995) 515.
- [17] Livsmedelsverket, Livsmedelstabell – Energi-och Näringsämnen 2002, Livsmedelsverket, Stockholm, 2002.
- [18] S. Carlström, C.-A. Ingemansson, Juvenile diabetes with long-standing remission, *Diabetologia* 3 (1967) 465.
- [19] R. Illig, A. Prader, Remission in juvenile diabetes, *Lancet* 30 (1968) 1190.
- [20] L. Ljung, *System Identification: Theory for the User*, second ed., Prentice-Hall, Upper Saddle River, NJ, 1999.
- [21] K.J. Åström, B. Wittenmark, *Computer-Controlled Systems*, third ed., Prentice-Hall, Upper Saddle River, NJ, 1997.
- [22] L.R.J. Haverkamp, *State space identification, theory and practice*, Ph.D. Thesis, Delft University of Technology, Delft, The Netherlands 2000.
- [23] M. Hanss, O. Nehls, Simulation of the human glucose metabolism using fuzzy arithmetic, in: *Fuzzy Inference Proceedings Society*, 2000, NAFIPS, 19th International Conference North America, 2000, p. 201.
- [24] M. Berger, D. Rodbard, Computer simulation of plasma insulin and glucose dynamics after subcutaneous insulin injection, *Diabetes Care* 12 (10) (1989) 725.
- [25] J. Brange, A. Vølund, Insulin analogs with improved pharmacokinetic profiles, *Adv. Drug Delivery Rev.* 35 (1999) 307.
- [26] D.R.L. Worthington, Minimal model of food absorption in the gut, *Med. Inform.* 22 (1) (1997) 35.
- [27] C. Dalla Man, A. Caumo, C. Cobelli, The oral glucose minimal model: estimation of insulin sensitivity from a meal test, *IEEE Trans. Biomed. Eng.* 49 (5) (2002) 419.
- [28] L. Heinemann, C. Weyer, M. Rauhaus, S. Heinrichs, T. Heise, Variability of the metabolic effect of soluble insulin and the rapid-acting insulin analog insulin aspart, *Diabetes Care* 21 (11) (1998) 1910.
- [29] D. Jenkins, T. Wolever, A. Jenkins, Starchy foods and glycemic index, *Diabetes Care* 11 (2) (1988) 149.
- [30] E. Ackerman, L. Gatewood, J. Rosevear, G. Molnar, Model studies of blood-glucose regulation, *Bull. Math. Biophys.* 27 (Special issue) (1965) 21.
- [31] L. Ljung, *System Identification Toolbox for Matlab*, MathWorks, 2002.
- [32] R. Diagnostics, *Accu-Check Compact Glucose* (07 2001).
- [33] E. Carson, T. Deutsch, H. Leicester, A. Roudsari, P. Sonksen, Challenges for measurement science and measurement practice: the collection and interpretation of home-monitored blood glucose data, *Measurement* (1998) 281.
- [34] R. Basu, B. Di Camillo, G. Toffolo, A. Basu, P. Shah, A. Vella, R. Rizza, C. Cobelli, Use of a novel triple tracer approach to assess postprandial glucose metabolism, *Am. J. Physiol. Endocrinol. Metab.* 284 (2003) E55.
- [35] B. Kovatchev, D. Cox, L. Gonder-Frederick, W. Clarke, Symmetrization of the blood glucose measurement scale and its applications, *Diabetes Care* 20 (1997) 1655.
- [36] J.B. Miller, Importance of glycemic index in diabetes, *Am. J. Clin. Nutr.* 59 (Suppl.) (1994) 747.
- [37] M. Gannon, F. Nuttall, Factors affecting interpretation of postprandial glucose and insulin areas, *Diabetes Care* 10 (6) (1987) 759.
- [38] F.X. Pi-Sunyer, Glycemic index and disease, *Am. J. Clin. Nutr.* 76 (Suppl.) (2002) 290S.
- [39] T.M.S. Wolever, D.J.A. Jenkins, The use of the glycemid index in predicting the blood glucose response to mixed meals, *Am. J. Clin. Nutr.* 43 (1986) 167.
- [40] S.K. Foster-Powell, J. Brand-Miller, International table of glycemic index and glycemic load values: 2002, *Am. J. Clin. Nutr.* 76 (2002) 5.
- [41] M. Kozek, N. Jovanovic, Identification of Hammerstein/Wiener nonlinear systems with extended Kalman filters, *Proc. Am. Control Conf.* (2002) 969.
- [42] Novo Nordisk AS, www.novonordisk.com.
- [43] Eli Lilly and Company, www.lilly.com.